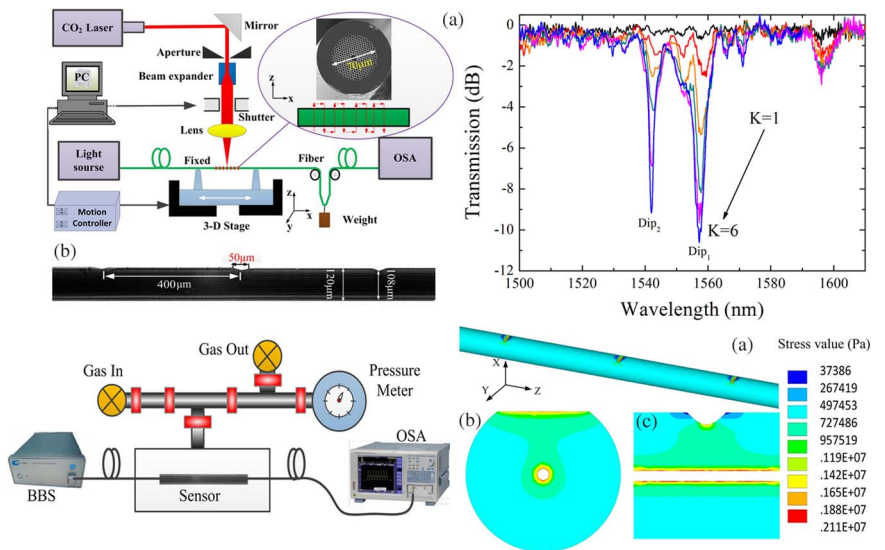


# Gas Pressure Sensor Based on CO<sub>2</sub>-Laser-Induced Long-Period Fiber Grating in Air-Core Photonic Bandgap Fiber

Volume 7, Number 5, October 2015

Jian Tang  
Guolu Yin  
Shen Liu  
Xiaoyong Zhong  
Changrui Liao  
Zhengyong Li  
Qiao Wang  
Jing Zhao  
Kaiming Yang  
Yiping Wang, Senior Member, IEEE



DOI: 10.1109/JPHOT.2015.2475636  
1943-0655 © 2015 IEEE

# Gas Pressure Sensor Based on CO<sub>2</sub>-Laser-Induced Long-Period Fiber Grating in Air-Core Photonic Bandgap Fiber

Jian Tang, Guolu Yin, Shen Liu, Xiaoyong Zhong, Changrui Liao, Zhengyong Li, Qiao Wang, Jing Zhao, Kaiming Yang, and Yiping Wang, *Senior Member, IEEE*

Key Laboratory of Optoelectronic Devices and Systems of Ministry of Education and Guangdong Province, College of Optoelectronic Engineering, Shenzhen University, Shenzhen 518060, China.

DOI: 10.1109/JPHOT.2015.2475636

1943-0655 © 2015 IEEE. Translations and content mining are permitted for academic research only. Personal use is also permitted, but republication/redistribution requires IEEE permission. See [http://www.ieee.org/publications\\_standards/publications/rights/index.html](http://www.ieee.org/publications_standards/publications/rights/index.html) for more information.

Manuscript received July 9, 2015; revised August 28, 2015; accepted August 28, 2015. Date of publication September 1, 2015; date of current version September 11, 2015. This work was supported in part by the National Natural Science Foundation of China under Grant 61425007, Grant 11174064, Grant 61377090, Grant 61575128, Grant 61308027, and Grant 61405128; by the Guangdong Provincial Department of Science and Technology under Grant 2014A030308007, Grant 2014A030312008, Grant 2014B050504010, Grant 2015B010105007, and Grant 2015A030310243; by the Science and Technology Innovation Commission of Shenzhen/Nanshan under Grant KQCX20120815161444632, Grant ZDSYS20140430164957664, Grant KC2014ZDJ0008A, and Grant GJHZ20150313093755757; by the China Postdoctoral Science Foundation Funded Project under Grant 2014M552227 and Grant 2015T80913; and by the Pearl River Scholar Fellowships. Corresponding author: Y. Wang (e-mail: ypwang@szu.edu.cn).

**Abstract:** We reported a gas pressure sensor based on CO<sub>2</sub>-laser-induced long-period fiber grating (LPFG) in an air-core photonic bandgap fiber (PBF). The LPFG was inscribed in an air-core PBF by the use of an improved CO<sub>2</sub> laser system with an ultraprecision 2-D scanning technique, which induced periodic collapses of air holes along the axis of the PBF. Such an LPFG could be used to develop a promising gas pressure sensor with a sensitivity of  $-137$  pm/MPa. Moreover, a simplified fiber model with a relatively similar elastic response was developed to qualitatively study the gas pressure response of the LPFG inscribed in the air-core PBF. A simulated stress distribution along the LPFG revealed that the gas pressure leads to a stress concentration at the collapsed area of the air holes in the fiber cladding, which finally results in a resonant wavelength shift of the LPFG through an elasto-optical effect.

**Index Terms:** Long period fiber gratings (LPFG), CO<sub>2</sub> lasers, photonic bandgap fibers, gas pressure sensors.

## 1. Introduction

Long period fiber gratings (LPFGs) inscribed in micro-structured fiber have been extensively explored for telecommunication and sensor applications [1]–[4]. Various inscription methods, including CO<sub>2</sub> laser irradiation [5]–[8], electric arc discharge [9], [10], and femtosecond laser exposure [11], [12], have been demonstrated to write LPFGs in different types of micro-structured fibers. However, most of them are index-guiding photonic crystal fibers (PCFs) or solid-core photonic bandgap fibers (PBFs) [13]–[16]. There has not been much research on LPFGs inscribed in air-core PBFs [17], [18]. Since almost of fundamental mode energy is confined in air-core region, it is

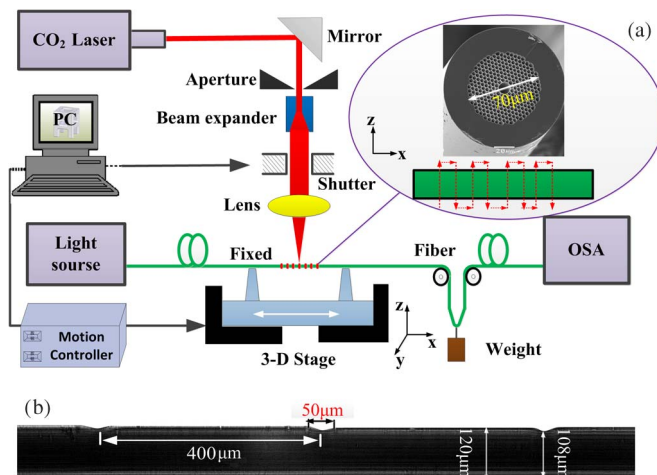


Fig. 1. (a) Experimental setup for LPFG inscription with an improved CO<sub>2</sub> laser beam scanning technique. (Inset) SEM of the used HC-PBF. (b) Side view of the obtained LPFG.

hard to induce periodic index modulation along the fiber axis direction. In 2008, Wang *et al.* first inscribed a LPFG in an air-core PBF by use of high frequency CO<sub>2</sub> laser irradiation to periodically collapse the cladding air holes [17]. In 2010, Iadicicco *et al.* proposed a pressure-assisted arc discharge technique to inscribe a LPFG in an air-core PBF by periodically modifying the hole size and shape in both air core and cladding region [18].

Thus far, the application investigations of LPFGs inscribed in an air-core PBF are very little. In literature [17], it has demonstrated that such LPFG with periodic collapse is highly sensitive to strain but insensitive to temperature and bend. Especially, the resonant wavelength and peak transmission hardly changed when such LPFG was immersed into different refractive index liquids with an index variation of 0.5 [17]. On the other hand, optical fiber gas pressure sensors currently are attracting significant interests in the area of sensing due to their potential advantages, such as multiplexing capability, compact size, immunity to electromagnetic interference and easy signal detection [19]. The tapered LPFGs inscribed in single mode fiber (SMF) for pressure measurement have been reported with a pressure sensitivity of 51 pm/MPa [20], but the temperature coefficient reaches up to 50 pm/°C. This existed temperature cross-sensitivity may limit its practical application scope. To solve this problem, tapered LPFGs written in PCFs were proposed with a pressure sensitivity of 112 pm/MPa and a negligible temperature sensitivity of about 0.3 pm/°C [21].

In this paper, we demonstrated a LPFG inscribed in an air-core PBF for gas pressure sensing. The LPFG was inscribed by use of an improved CO<sub>2</sub> laser beam scanning technique, which greatly enhanced the writing efficiency and repeatability. The gas pressure performance of this kind sensor was experimentally investigated. The corresponding theoretical analysis was also studied by use of the ANSYS software.

## 2. LPFG Inscription in Air-Core PBF

The fabrication setup we used as shown in Fig. 1(a), such a system consisted of an industrial CO<sub>2</sub> laser (SYNRAD 48-1) with a maximum power of 10 W. The output laser beam diameter was first expanded by a four times beam expander and was then focused on a spot of 35 µm in diameter with a 63.5 mm focal-length infrared lens. An electric shutter was used for turning on/off the laser beam. In order to realize a two-dimensional scanning as shown in the inset of Fig. 1(a), we specifically designed a computer control program with LabVIEW software to control a three-dimensional ultra-precision translation stage. It is worth pointing out that the power stability of the CO<sub>2</sub> laser was improved to ±2% by use of a closed loop control system.

Compared with the CO<sub>2</sub> laser power fluctuates up to  $\pm 10\%$  employed in literature [17], the larger improvement of power stability is one of the main factors to write high-quality LPFGs in air-core PBFs.

An air-core PBF (HC-1500-02 PBF from Crystal Fiber) was employed to inscribe a LPFG, as shown inset of Fig. 1(a). In the fiber, the air core has a diameter of  $10.9\ \mu\text{m}$  and is surrounded by a holey lattice with an average pitch value of  $3.8\ \mu\text{m}$ . The holey cladding region has a diameter of  $70\ \mu\text{m}$  and is surrounded by a ring of solid silica. The total diameter of the fiber is about  $120\ \mu\text{m}$ . The thickness of the silica bridges between cladding-holes is only about  $0.34\ \mu\text{m}$ , and the air-filling fraction of holey cladding region is above 90%, which means that the air holes are easy to collapse when such a PBF is spliced to other optical fibers.

First of all, each end of the PBF with a length of 5 cm was spliced to a single mode fiber by use of a commercial fusion splicer (FSM-60) with a manual mode. During splicing the air-core PBF, the end face of the PBF was placed at the region far away from the arc discharge center in order to avoiding collapse the air holes. The fusion parameters such as arc power, arc time and pushing distance were improved to reduce the splice losses and weaken the interference between the fundamental mode and surface modes. An optimized arc power, i.e., stander-60, and an arc time of 400 ms were used in our experiment. Consequently, a low splice loss of about 3.5 dB was realized, and the splice joint exhibited a good mechanical strength.

When we inscribed a LPFG in an air-core PBF, the coating of the PBF was stripped off and then was placed in the focal plane of the CO<sub>2</sub> laser beam. One of the fiber ends was fixed by a fiber holder, a small weight of 5 g was attached to the other end to keep the fiber straight and provide a constant pre-strain in the fiber. During the fabrication process, the output laser power is 200 mW and the spot size is about  $35\ \mu\text{m}$ . As shown the red arrow in the inset of Fig. 1(a), the focused CO<sub>2</sub> laser beam was first scanned along the “Z” direction and was then shifted by a grating period, e.g.,  $400\ \mu\text{m}$ , along the “X” direction, i.e., the fiber axis, and then moved by 1 mm along the “-Z” direction in order that the focused CO<sub>2</sub> laser beam scans/irradiates cross the fiber again [7]. This scanning and shifting process was periodically carried out for  $N$  ( $N$  is the number of grating periods) times, e.g., 30 times, which is called one scanning cycle. The above process were repeated for  $K$  ( $K$  is the number of scanning cycles) cycles until a desired LPFG is achieved [22]. Fig. 1(b) shows the microscope image of the LPFG with periodic collapse face to the CO<sub>2</sub> laser exposure side. The width and depth of the collapsed region are  $50\ \mu\text{m}$  and  $12\ \mu\text{m}$ , respectively. A broadband light source (BBS, NKT Photonics SuperK) and an optical spectrum analyzer (OSA, YOKOGAWA AQ6370C) with a resolution of 0.02 nm were employed to monitor transmission spectrum evolution during we increased the number of scanning cycles from 1 to 6 (see Fig. 2). Two resonant dips have been found at resonant wavelengths of 1555.91 (Dip<sub>1</sub>) and 1541.41 nm (Dip<sub>2</sub>), respectively. We suspect that a two-step process could be involved: the fundamental core mode is coupled to discrete higher order (core or surface-like) modes and then to lossy quasi-continuum of cladding and radiating modes [17], [23]. The depth of the two resonant dips gradually increased with an increase of scanning cycle, and finally reached to  $-10.61\ \text{dB}$  and  $-9.15\ \text{dB}$ , respectively.

During our LPFG fabrication process, only six scanning cycles were required. Compared with fifty scanning cycles are needed in literature [17], the writing efficiency was greatly improved in our fabrication technology. This improvement mainly attributes to the excellent power stability of the CO<sub>2</sub> laser ( $\pm 2\%$ ). The relatively low power fluctuation improves the uniformity of the periodic collapse along the fiber axis, which enhances the mode coupling at the resonant wavelength. Hence, a LPFG with relative large depth at the resonant dip is expected by use of fewer scanning cycles.

### 3. Experimental Results

The gas pressure response of the LPFG was tested by using the experimental setup, as shown in Fig. 3. The pressure measurements were performed at room temperature. The inscribed LPFG sample was fixed on a short piece of steel ribbon to keep the fiber grating straight. Then,

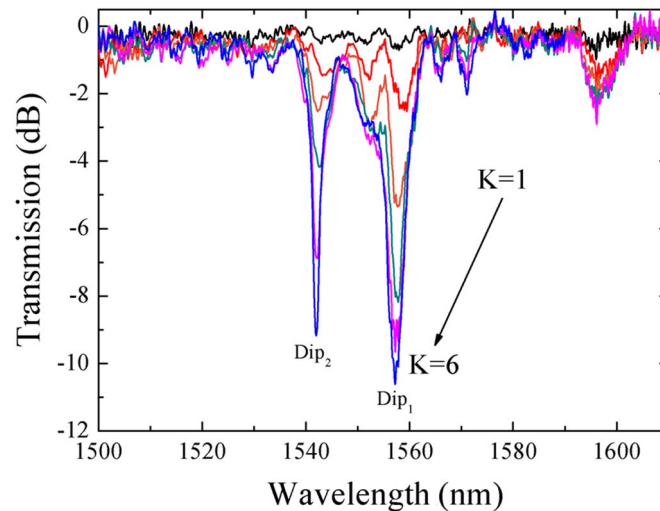


Fig. 2. Transmission spectrum evolution of a LPFG with 30 grating periods and a grating pitch of  $400 \mu\text{m}$  while the number of scanning cycles ( $K$ ) increases from 1 to 6.

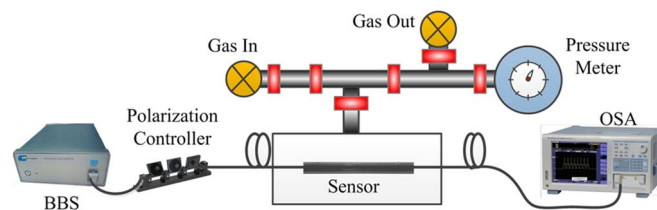


Fig. 3. Experimental setup for gas pressure measurement.

it was placed into a gas chamber, where a commercial gas pressure generator with a stability of  $\pm 0.2$  KPa is equipped with a high-precision digital pressure meter (ConST-811) to measure the pressure in the chamber. The chamber was fitted with a feed-through and sealed by strong glue to extend the fiber pigtail outside the chamber for real-time measurement. The pressure in the chamber was increased from 0 to 2.4 MPa with an interval of 0.4 MPa, staying for about ten minutes at each step to observe the stability of the spectrum. Due to the single-side  $\text{CO}_2$  laser exposure to air-core PBF during inscription of the gratings, the achieved LPFG has a large polarization dependent loss as high as 25 dB [17], which indicates that the transmission spectrum varies with the input polarization state of the light waves. A polarization controller was employed to minimize the influence of polarization state on the gas pressure measurements. We adjusted the polarization controller until the depth of the resonant dips reached a maximum value before gas pressure measurements. In addition, the fiber outside of the gas chamber was taped in order to better maintain the polarization state.

In our experiment, the gas pressure characteristics of  $\text{Dip}_1$  and  $\text{Dip}_2$  are respectively monitored for better understanding pressure response of the LPFGs written in the air-core PBF. As shown in Fig. 4(a) and (b), both  $\text{Dip}_1$  and  $\text{Dip}_2$  shift toward shorter wavelengths with the pressure increasing gradually from 0 to 2.4 MPa with an interval of 0.4 MPa. The relationship between resonant wavelength  $\lambda$  and gas pressure  $P$  was shown in Fig. 5. The fitting curves can be expressed as  $\lambda_1 = -0.137 \cdot P_1 + 1556.04$  for  $\text{Dip}_1$  and  $\lambda_2 = -0.088 \cdot P_2 + 1541.50$  for  $\text{Dip}_2$ . The fitting degrees  $R^2 = 0.997$  and  $0.996$  exhibit a linear wavelength response to the gas pressure. The experiment sensitivity of  $\text{Dip}_1$  and  $\text{Dip}_2$  are  $-137$  pm/MPa and  $-88$  pm/MPa, respectively.



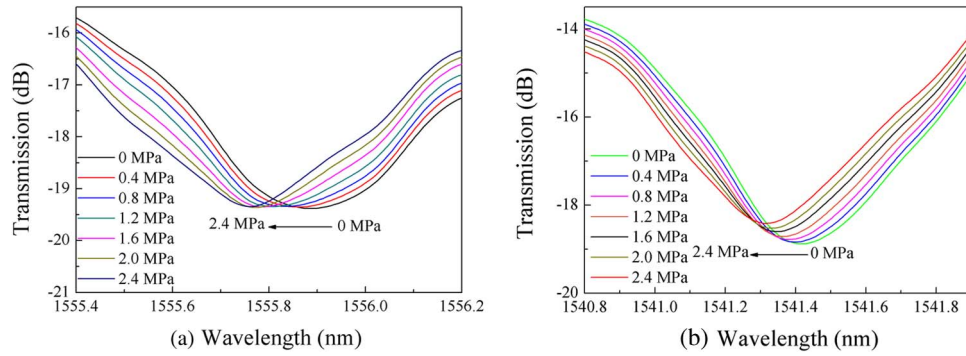


Fig. 4. Transmission spectrum evolution of (a) Dip<sub>1</sub> and (b) Dip<sub>2</sub> while the gas pressure increases from 0 to 2.4 MPa.

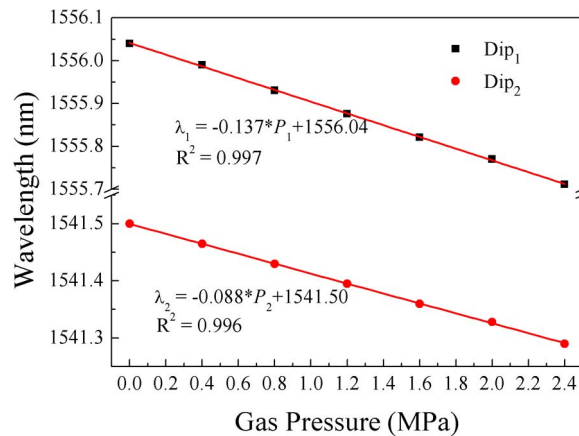


Fig. 5. Relationship between gas pressure and resonant wavelength of Dip<sub>1</sub> and Dip<sub>2</sub> while the gas pressure increases from 0 to 2.4 MPa.

Periodically tapered LPFGs in the SMF and PCF have been employed for gas pressure sensing in [20] and [21], in which the gas pressure measurement interval of the tapered LPFGs in SMF and PCF were 15 MPa and 6 MPa, respectively. It indicates that the tapered LPFGs in SMF and PCF are not suitable to being used to sense a low gas pressure. In contrast, our proposed PBF-based sensors can be used to measure a low gas pressure of less than 0.5 MPa. The reason for this is that it is easier to induce a physical deformation in an air-core PBF than in a solid-core SMF and PCF.

#### 4. Discussion

As we known, the increase of gas pressure would result in the air refractive index variation [18]. To evaluate the influence of the index variation on the gas pressure sensor, we immersed the LPFG into a series of commercial refractive index matching liquids (Cargille Lab, <http://www.cargille.com>) ranging from 1.30 to 1.45 with a step of 0.01. We found that both resonant wavelength and peak transmission attenuation hardly changed. It means that the LPFG in an air-core PBF is insensitive to the variation of external refractive index. On the other hand, when the pressure is changed from 0 to 2.4 MPa, the air index variation is only 0.006 RIU [18], which is much smaller than the refractive index variation of the matching liquids. Therefore, we have reason to believe that the tiny change in air index caused by the air compression cannot lead to the wavelength shift of the resonant dip.

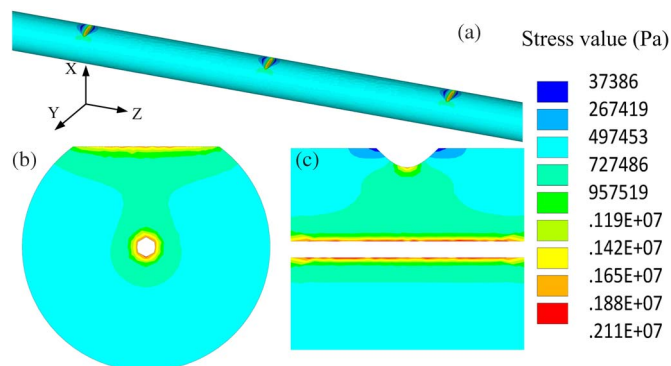


Fig. 6. (a) Simplified 3-D model of air-core fiber. (b) Transverse stress contour at the center of collapsed area. (c) Longitudinal stress contour around the collapsed area, where the Young's modulus of silica is 73 GPa, Poisson's ratio is 0.17, and silica density is 2700 Kg/m<sup>3</sup>.

Here, the gas sensing mechanism can be qualitatively explained by the stress distribution when gas pressure is applied on the single-side collapsed air-core PBF. For better illustrating this condition, a three dimensional simulation model is established by use of ANSYS as shown in Fig. 6(a). It is extremely hard to construct a real air-core PBF model with multi-air holes in ANSYS, hence, we simplified the air-core PBF into a silica tube with a 10  $\mu\text{m}$  air core. Periodical grooves with a pitch of 400  $\mu\text{m}$  are carved in the tube to represent the periodical collapses in an air-core PBF. The width and depth of the carved area are 50  $\mu\text{m}$  and 12  $\mu\text{m}$ , which are equal to the experimental values of the collapsed areas. Fig. 6(a)–(c) illustrate the stress contour profile in the three-dimension view, transverse view at the groove area, and the longitudinal view when we applied a pressure of 1 MPa. The simulation parameters are as follows: the Young's modulus of silica is 73 GPa, Poisson's ratio is 0.17, silica density is 2700 Kg/m<sup>3</sup>. The blue and red areas represent the min and max stress value, respectively. It evidently demonstrates that outer air pressure can lead to a stress concentration at the collapsed area and then transfer into the air-hole. Thus the stress concentration modifies the sizes and the shapes of the microstructure cladding cells and hollow core. Meanwhile it changes the refractive index of silica material through elasto-optical effect. Both the change of geometry and the refractive index lead to a effective refractive indices variation of fiber modes in an air-core PBF and finally lead to a shift of the resonant wavelength.

## 5. Conclusion

We experimentally demonstrated a gas pressure sensor based on a CO<sub>2</sub>-laser-induced LPFG in an air-core PBF. Single-side periodic collapses were produced to inscribe a LPFG by use of a CO<sub>2</sub> laser system with two-dimensional scanning technique. Due to excellent CO<sub>2</sub> laser power stability and ultra-precision translation stage, we achieved a high-quality LPFG with only six scanning cycles of CO<sub>2</sub> laser beam, which exhibits high inscription efficiency of gratings. Such a LPFG with periodic collapses could be developed a promising gas pressure sensor with a sensitivity of  $-137$  pm/MPa. The gas pressure response mechanism is due to the gas-pressure-induced stress concentration at the collapse region of the LPFG. We expect that such a gas pressure sensor would find potential applications in the field of sensing.

## References

- [1] G. Kakarantzas, T. A. Birks, and P. S. Russell, "Structural long-period gratings in photonic crystal fibers," *Opt. Lett.*, vol. 27, no. 12, pp. 1013–1015, Jun. 2002.
- [2] K. Morishita and Y. Miyake, "Fabrication and resonance wavelengths of long-period gratings written in a pure-silica photonic crystal fiber by the glass structure change," *J. Lightw. Technol.*, vol. 22, no. 2, pp. 625–630, Feb. 2004.

- [3] J. Jian, J. Wei, and H. H. Lut, "Compact in-fiber interferometer formed by long-period gratings in photonic crystal fiber," *IEEE Photon. Technol. Lett.*, vol. 20, no. 23, pp. 1899–901, Dec. 2008.
- [4] L. Rindorf and O. Bang, "Highly sensitive refractometer with a photonic-crystal-fiber long-period grating," *Opt. Lett.*, vol. 33, no. 6, pp. 563–565, Mar. 2008.
- [5] X. Zhong *et al.*, "High-sensitivity strain sensor based on inflated long period fiber grating," *Opt. Lett.*, vol. 39, no. 18, pp. 5463–5466, Sep. 2014.
- [6] Y.-P. Wang, L. Xiao, D. N. Wang, and W. Jin, "Highly sensitive long-period fiber-grating strain sensor with low temperature sensitivity," *Opt. Lett.*, vol. 31, pp. 3414–3416, Dec. 2006.
- [7] X. Zhong *et al.*, "Long period fiber gratings inscribed with an improved two-dimensional scanning technique," *IEEE Photon. J.*, vol. 6, no. 4, Aug. 2014, Art. ID. 2201508.
- [8] Y. P. Wang, Y. J. Rao, Z. L. Ran, and T. Zhu, "Unique characteristics of long-period fibre gratings fabricated by high-frequency CO<sub>2</sub> laser pulses," *Acta Phys. Sin.*, vol. 52, pp. 1432–1437, Jun. 2003.
- [9] G. Yin *et al.*, "Long period fiber gratings inscribed by periodically tapering a fiber," *IEEE Photon. Technol. Lett.*, vol. 26, no. 7, pp. 698–701, Apr. 2014.
- [10] G. Humbert, A. Malki, S. Fevrier, P. Roy, and D. Pagnoux, "Electric arc-induced long-period gratings in Ge-free air-silica microstructure fibres," *Electron. Lett.*, vol. 39, no. 4, pp. 349–350, Feb. 2003.
- [11] L. Shujing *et al.*, "Structural long period gratings made by drilling micro-holes in photonic crystal fibers with a femtosecond infrared laser," *Opt. Exp.*, vol. 18, no. 6, pp. 5496–5503, Mar. 2010.
- [12] C. Florea and K. A. Winick, "Fabrication and characterization of photonic devices directly written in glass using femtosecond laser pulses," *J. Lightw. Technol.*, vol. 21, no. 1, pp. 246–253, Jan. 2003.
- [13] H. Dobb, K. Kalli, and D. J. Webb, "Measured sensitivity of arc-induced long-period grating sensors in photonic crystal fibre," *Opt. Commun.*, vol. 260, no. 1, pp. 184–191, Apr. 2006.
- [14] C.-L. Zhao, L. Xiao, J. Ju, M. S. Demokan, and W. Jin, "Strain and temperature characteristics of a long-period grating written in a photonic crystal fiber and its application as a temperature-insensitive strain sensor," *J. Lightw. Technol.*, vol. 26, no. 2, pp. 220–227, Jan./Feb. 2008.
- [15] H. W. Lee and K. S. Chiang, "CO<sub>2</sub> laser writing of long-period fiber grating in photonic crystal fiber under tension," *Opt. Exp.*, vol. 17, no. 16, pp. 4533–4539, Mar. 2009.
- [16] L. Changrui, W. Ying, D. N. Wang, and J. Long, "Femtosecond laser inscribed long-period gratings in all-solid photonic bandgap fibers," *IEEE Photon. Technol. Lett.*, vol. 22, no. 6, pp. 425–427, Mar. 2010.
- [17] Y. Wang *et al.*, "Long period gratings in air-core photonic bandgap fibers," *Opt. Exp.*, vol. 16, no. 4, pp. 2784–2790, Feb. 2008.
- [18] A. Iadicicco, S. Campopiano, and A. Cusano, "Long-period gratings in hollow core fibers by pressure-assisted arc discharge technique," *IEEE Photon. Technol. Lett.*, vol. 23, no. 21, pp. 1567–1569, Nov. 2011.
- [19] Z. Li *et al.*, "Highly-sensitive gas pressure sensor using twin-core fiber based in-line Mach-Zehnder interferometer," *Opt. Exp.*, vol. 23, no. 5, pp. 6673–6678, Mar. 2015.
- [20] W. J. Bock, J. Chen, P. Mikulic, and T. Eftimov, "A novel fiber-optic tapered long-period grating sensor for pressure monitoring," *IEEE Trans. Instrum. Meas.*, vol. 56, no. 4, pp. 1176–1180, Aug. 2007.
- [21] W. J. Bock, J. Chen, P. Mikulic, T. Eftimov, and M. Korwin-Pawlowski, "Pressure sensing using periodically tapered long-period gratings written in photonic crystal fibres," *Meas. Sci. Technol.*, vol. 18, no. 10, pp. 3098–3102, Oct. 2007.
- [22] Y.-P. Wang, D. N. Wang, W. Jin, Y.-J. Rao, and G.-D. Peng, "Asymmetric long period fiber gratings fabricated by use of CO<sub>2</sub> laser to carve periodic grooves on the optical fiber," *Appl. Phys. Lett.*, vol. 89, Oct. 2006, Art. ID. 151105.
- [23] L. Jin, W. Jin, J. Ju, and Y. Wang, "Investigation of long-period grating resonances in hollow-core photonic bandgap fibers," *J. Lightw. Technol.*, vol. 29, no. 11, pp. 1708–1714, Jun. 2011.